

This manuscript was presented at the Boundary Layer Wind
Tunnel Laboratory at the University of Western Ontario,
April 8, 1987

THE WAVES PROGRAMME
ON
THE CCIW RESEARCH TOWER

by
I.K. Tsanis¹ and M.A. Donelan²

¹ Visiting Fellow, NWRI

² Research and Applications Branch
National Water Research Institute
Canada Centre for Inland Waters
867 Lakeshore Road, P.O. Box 5050
Burlington, Ontario, Canada L7R 4A6

May 1987

ABSTRACT

The Canada Centre for Inland Waters Research Tower is positioned in 12 m of water, 1.1 km off the beach at the west end of Lake Ontario near Hamilton, Ontario and is used for wave and air-water interaction research. The instrumental and computational facilities, including the principle and purpose of the various sensors, the data acquisition system and the data gathering processes are briefly described.

RÉSUMÉ

La tour du Centre canadien de recherche sur les eaux intérieures est placée dans 12 m d'eau, à 1,1 km de la côte ouest du lac Ontario près de Hamilton (Ontario) et est utilisée pour des recherches sur les vagues et les interactions air-eau. On décrit brièvement les instruments et les méthodes informatiques utilisées, c'est-à-dire le principe et le rôle des divers capteurs et le système d'acquisition des données ainsi que les méthodes utilisées dans ce domaine.

1.0 INTRODUCTION

The Great Lakes are Canada's most precious fresh water resource, and play an important role in meeting human needs for supplying water, sources of food, energy and places of recreation. With the rapid increase in population growth in the Great Lakes basin (from 30,000 to 40 million in the last 170 years) and the rapid increase of industrialization in the last 40 years, ever more pollutants have been introduced into the lakes causing serious problems in water quality. Detailed knowledge of the hydrodynamic processes (for example, mixing) is necessary because essential elements for life and productivity such as oxygen, heat and nutrients are transported and dispersed through these processes.

The hydrodynamic behaviour of lakes is largely determined by their geometry. Although most lakes are much smaller than the oceans resulting in a negligible effect of astronomical tides, they are large enough for a significant Coriolis effect to become apparent. Although the system can gain or lose mass from inflows and outflows such as rivers, and circulations may be induced by density gradients due to seasonal temperature differences, the principal source of mechanical energy is the wind, which is applied on the principal boundary, the free surface or the air-water interface. Knowledge of the physical processes at the air-water interface that affect the exchanges of momentum, heat, water vapor and pollutant transfer at the air-water interface is essential in order to develop methods for further improvement of water quality.

The CCIW Research Tower provides a stable platform for limnological observations and field studies of physical processes at the air-water interface. Since 1976 a research programme of Water Air Vertical Exchange Studies (WAVES) has been conducted from the tower. Other scientific and engineering experiments can be undertaken, for example wind-wave loading of offshore structures. The latter is one of the main themes of the present five-year research project (1985 - 1990)

entitled "Deep-Water Wave Breaking and Wave-Turbulence Interaction" which is a joint project between mainly the Canada Centre for Inland Waters and the Woods Hole Oceanographic Institution (WHOI). The Finnish Institute of Marine Research (FMR) and John Hopkins University (JHU) also participate in this study and the United States Naval Research Laboratory (NRL) is involved with radar scattering experiments having a bearing on satellite remote sensing of surface winds over the oceans. The CCIW Research Tower, its instrumentation and the data acquisition system will be described briefly.

2.0 DESCRIPTION OF THE TOWER

Figure 1 shows a map indicating the location of the research tower, the CCIW and the shore-normal profile in the vicinity of the tower. Overall views of the tower with the various sensors used for data collection in this research project are shown in Figures 2 and 3, which are taken from the north-west and south-east directions, respectively. The spikes at the corners of the tower are lightning arresters.

The tower stands in approximately 12 m of water on piles driven to bed-rock. The structure supports 100 square metres of upper deck and the legs (of diameter 40 cm) are angled at 10 degrees. The upper deck is an open grating in order to let snow and rain through and to impose less resistance to the wind. The low walkway is approximately 4 m from the water level. The design wave was 7 m with an 8 sec period. The resonance frequency of the structure is such that it is only excited to resonance by waves of about 0.5 m in height so the large waves are nearly transparent to it. Electrical power (6 KW at 600 V) is carried to the tower by underwater cable.

The white structure on the top of the tower is the data acquisition system housing. On the top center of the tower there is a Gill-type anemometer-bivane, which measures the vertical and horizontal components of the wind. Beside it are the fast acting temperature

and humidity sensors. These together yield fluxes of momentum, heat and water vapor. The structure to the right is an elevator handling the turbulence array which is used to measure dynamic and static pressure above the waves to yield information about wave generation and attenuation by wind. An array of wave staffs of 4.8 mm in diameter is visible to the right of center. This is used to yield wave direction information. In front of it is a single miniature wave staff, of 1.1 mm in diameter which provides more detailed information of the water surface elevation. Boarding access to the tower is shown in Figure 4.

3.0 WIND PROFILER

Figure 5 is a close-up view of the elevator handling the turbulence array which is called the wind profiler. The grey object on the top is the motor and gear box that drive the elevator up and down by computer control. The black curved item is the cable trough that keeps the elevator cables from blowing around in the wind. The array is faced into the wind by the tail fin, and the square box holds the electronics, the pressure transducers and the pneumatic filters. At the bottom of the pivot is the damping system containing silicone oil, which keeps it from oscillating. Below that is the wave staff for measuring the wave height for correlation with pressure and wind speed. Figure 6 shows the inside of the box, which contains six pressure transducers, and three pneumatic capacitance resistance networks. The latter reject the slow atmospheric pressure changes from the static pressure measurements.

A close-up view of the pitot tube and E-V probe is shown in Figure 7. The E-V probe is a small disk 4 cm in diameter which is contoured to a precise shape and has ports on either side that communicate with the upper and lower pieces of tubing. The original design is due to J. Elliott with manufacturing modifications due to G. Voros. The center of the unit is dished to reject dynamic pressure contamination for yaw angles up to ± 12 degrees. The tail keeps the array oriented to the average wind. The pitot tubes and E-V probes are

back-purged with dry nitrogen between measurements.

Figure 8 shows the X-film anemometer and cold-wire thermometer that are used to provide information on the stresses and heat fluxes close to the interface. These can be covered and uncovered by means of a pneumatic cylinder. The angles can be set to the angles used in the laboratory calibration by using the small protractor bonded to the side of the unit.

4.0 ROTATOR

Figures 9 and 10 show upper and side views of the rotator that was used to orient the water velocity sensors perpendicular to the oncoming waves. The rotator can rotate through 270 degrees. It extends to 7 m below water level and is supported with a plastic sleeve bearing. The Woods Hole BASS system is at the left hand side looking out from the tower, see Figure 9. The drag spheres are at the right hand side (below water level) but are not visible. Two wave staffs give water elevation data. The two wave staffs on either side of the rotator are shown in Figure 10.

The BASS unit is shown in Figure 11. This acoustic time of flight meter measures the transit time of an acoustic pulse between pairs of sensors arranged diagonally across the sampled volume. This sensor allows one to get three-dimensional measurements of the current velocity. The averaging area is large so this unit responds to fluctuations below about 2 Hz. Twelve of these are mounted on the rotator spaced vertically 50 cm apart.

Figure 12 shows the sensing element of the drag sphere. It is a 4 mm bead on a stalk that is mounted inside the unit on an invar cross. Strain gauges are mounted to the cross that give output signals for the x, y and z axes of the drag from which velocity components are computed. It is a square law device. The housing is filled with silicone oil and this keeps everything electrically isolated. The sleeve is extendable by pneumatic cylinder and covers the drag sphere

for mechanical protection and for determination of the zero speed readings. The unit is delicate but allows high frequency (up to 20 Hz) components to be measured and gives high accuracy and sensitivity to x and z axes (downwave and vertical).

5.0 OTHER SENSORS AND EXPERIMENTAL DEVICES

An array of six wave staffs, each 4.8 mm in diameter, which are arranged in a pentagon with one at the center for measuring directional spectra of waves, is shown in Figure 13. The wave staffs are capacitance gages and are held taut with rubber shock cords.

Figure 14 shows the WOODS HOLE Laser Doppler Velocimeter (LDV) on its elevator. It is bracketed out from the North-West corner of the tower and is movable in the vertical through about 1 m. It measures two components of velocity. Attached to the leg is the temperature profiler, which traverses from 6 m depth to the surface. Below the LDV on a 3 m boom, 7 m below the lake surface is an instrument called an Inverted Ecosounder, that looks upwards and samples in two channels at different frequencies, one of the order of kHz and one of the order of MHz. The reflected echos from dirt particles and air bubbles are binned by the mechanism to give range and vertical velocities by measuring time delay and doppler shift. At the moment it cannot yield horizontal velocities. It is able, though, to distinguish between air bubbles and dirt particles. It can also measure concentrations of bubbles in waves at different depths and their vertical velocities.

Three sets of radars from the United States Naval Research Laboratory are shown in Figure 15. These microwave scatterometers run at three different frequencies between 5 GHz and 35 GHz and measure radiation polarized in two directions that is scattered from the water surface back to the unit. They are operated in radar wave lengths of 9 mm to 6 cm, which is the range of the capillary gravity waves.

Figure 16 is a close-up view of the Gill anemometer-bivane, which measures horizontal and vertical wind directions and wind speed.

It has an effective frequency response of about 5 Hz. The air temperature (thermistor) and humidity sensors are also visible. The temperature sensor is attached to the bivan's support and is covered in order to reduce solar radiation errors. The capacitance-type humidity sensor ("Humicap") is mounted beneath the plate at the top of the tower.

The water temperature sensor, which measures near surface temperature, is shown in Figure 17. The bucket with a lid has a small hole in the bottom and an annular opening between the lid and the top of the bucket. The temperature sensor is inside the bucket. As a wave passes, the bucket fills with water, drains slowly and refills again, thereby keeping the sensor always wet and giving the temperature corresponding to the top 10 cm of water.

6.0 DATA ACQUISITION

A view of the inside of the data acquisition housing is shown in Figure 18. The data acquisition provides on-shore logging, display and pre-processing of data collected on the platform. The data are digitized on the tower and communicated by underwater cable to the data acquisition system, which is housed in a trailer on shore. The interfaces are visible to the left, the power supplies at the bottom right and the IBM-PC microcomputer on the right. The signals are filtered and amplified in the analog interface, digitized at 20 Hz and passed through a system of modems to an IBM-PC AT on shore. There the data are written on a 30 Mb hard disk. There are 48 channels in total.

Figure 19 shows the shoaling waves with the CCIW tower in the background. A view of the trailer is given in Figure 20 and a view of the instrumental and computational facilities used for data gathering in Figure 21. From the left to the right are (a) a telescope to view the tower, (b) a six-channel Gould tape recorder, (c) a FX-85 Epson dot matrix printer, (d) a Gandalf modem, (e) an IBM-PC AT microcomputer with

its keyboard and monitor, (f) a digital cassette recorder, (g) analog filters, (h) Waverider receivers and (i) two-channel Gould recorder. The 20 Hz digitized data from 48 channels is written on the hard disk. 80 minutes of data are collected in order to assure convergence of the turbulence quantities and adequate wave statistics. Before and after the runs 5 minutes of data are collected with the drag spheres covered in order to establish the drag sphere zeros. Each run requires 7 Mbs. After four runs the hard disk is full and the data is copied onto 40 Mb digital tapes via a digital tape drive. The disk is emptied and the logging process continues. The data from the Waverider is received by the Waverider receivers and copied on the cassette recorder at 2Hz frequency.

The Waveriders were placed by the scientific ship Limnos at 3 km and 20 km from shore aligned with the tower along the normal (240°) to the shore (see Figure 1). The front view of the Limnos with the service crane used for loading the equipment is shown in Figure 22. A Waverider (see Figure 23) is a buoy that follows the movements of the water surface and measures waves by measuring the vertical acceleration of the buoy. The Waverider is moored with an in-line 10 m rubber cord to permit it to follow the water surface. The procedure of launching the Waverider is shown in Figure 24 while Figure 25 shows a close-up view of the Waverider.

7.0 CALIBRATION

Figure 26 shows an overall view of the towing tank and carriage used to calibrate the drag spheres in water and the anemometer-bivane in air. The arrangement used for dynamic calibration (phase and amplitude response) of the pressure transducers (pitot tubes and E-V) is shown in Figure 27. A speaker, driven by an amplifier and a sine wave generator, pressurizes the cylindrical chamber in which the probe under test and a very fast pressure transducer are installed. Figure 28 shows the wind tunnel used for X-film calibration and for

experiments over solid wavy boundaries. The wave staffs were calibrated both in the laboratory and on the tower by raising and lowering them through measured distances with respect to a calm surface. All temperature sensors were calibrated in precisely controlled baths in our calibration facility at NWRI. The humidity sensor was calibrated using a controlled humidity chamber.

All the calibrations were carried out both before and after field exposure.

Figure 29 shows the ship "Shark", which was used to dismantle and remove all the sensors for the winter period.

Figures 30 and 31 show most members of the team of scientists, engineers, technicians and divers that was involved with this project during the fall of 1986.

Finally Figure 32 shows the waves breaking on shore on a cold November morning. As a part of our contribution this year we hope to bring better understanding to the physical processes involved in wave generation by wind and in deep-water wave breaking.

PERSONNEL

The list of people who contributed to this work is very long. The following is a list of major contributors in alphabetical order.

CCIW: S. Beal, D. Beesley, J. Cooper, Y. Desjardins, R. Desrosiers, J. Dolanski, M. Donelan, J. Ford, N. Madsen, M. Pedrosa, L. Peer, H. Savile, M. Skafel, B. Taylor, I. Tsanis, J. Valdmanis

FMR: K. Kahma

JHU: S. Kitaigorodskii

NRL: M. Evers, W. Keller, W. Plant

WHOI: Y. Agrawal, C. Belting, B. Brumley, C. Converse, F. Dias, P. Heuchling, E. Terray, A. Williams III

ACKNOWLEDGEMENTS

The experiment was supported in part by the Panel for Energy Research and Development under OERD project number 62114.

LIST OF FIGURE CAPTIONS

- Figure 1: Map showing the location of the research tower.
- Figure 2: A view of the tower from the north-east direction.
- Figure 3: A view of the tower from the south-east direction.
- Figure 4: The boat and the boarding ladder.
- Figure 5: A view of the wind profiler.
- Figure 6: The wind profiler's box with the filters and transducers.
- Figure 7: The E-V probe and the pitot tube.
- Figure 8: The X-film and cold-wire anemometers.
- Figure 9: An upper view of the rotator.
- Figure 10: A side view of the rotator.
- Figure 11: The BASS unit.
- Figure 12: The drag sphere.
- Figure 13: The wave staffs array.
- Figure 14: The laser doppler anemometer.
- Figure 15: Three sets of radars.
- Figure 16: The Gill anemometer-bivane.
- Figure 17: The water temperature sensor.
- Figure 18: A view of the inside of the data acquisition housing.
- Figure 19: Shoaling waves with the CCIW tower in the background.
- Figure 20: A view of the trailer.
- Figure 21: A view of the facilities in the trailer.

LIST OF FIGURE CAPTIONS (cont.)

- Figure 22: A view of the scientific ship "LIMNOS".
- Figure 23: The Waverider.
- Figure 24: Launching of the Waverider.
- Figure 25: The Waverider on the water surface.
- Figure 26: The towing tank facility.
- Figure 27: Equipment used for dynamic calibration of the pressure transducers.
- Figure 28: The wind tunnel.
- Figure 29: The ship "SHARK".
- Figure 30: The WAVES team on the tower.
- Figure 31: The team of scientists, engineers and technicians.
- Figure 32: The waves breaking on shore.

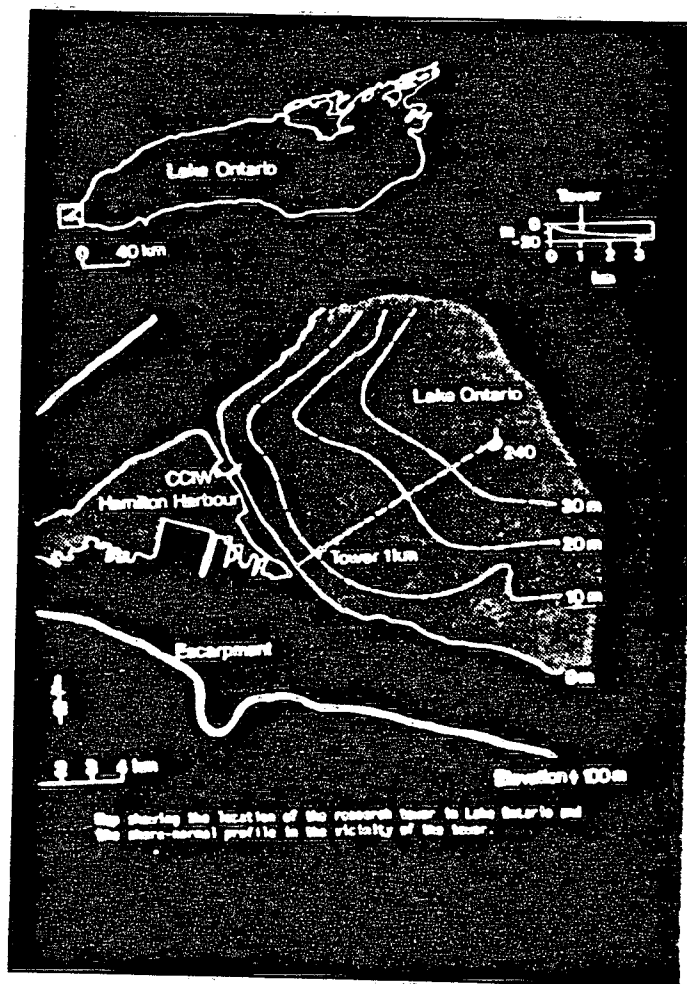


Figure 1

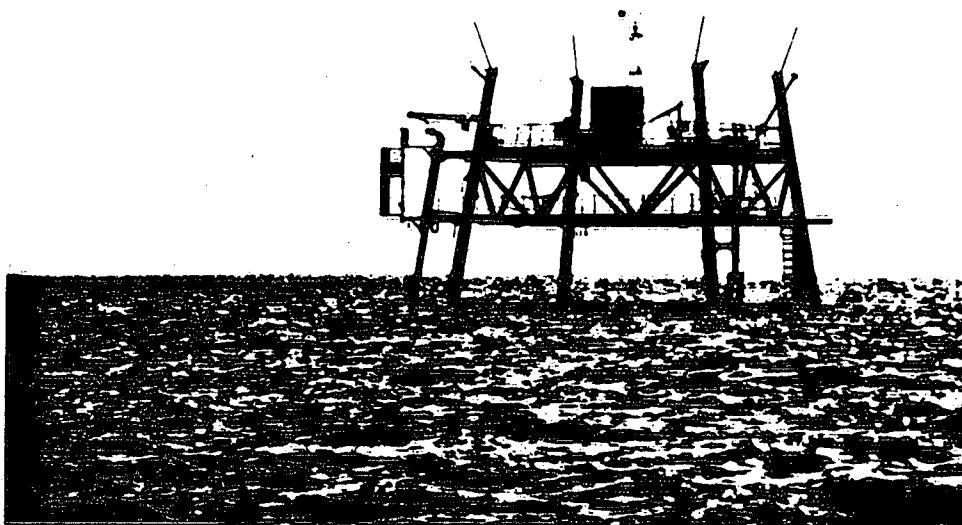


Figure 2

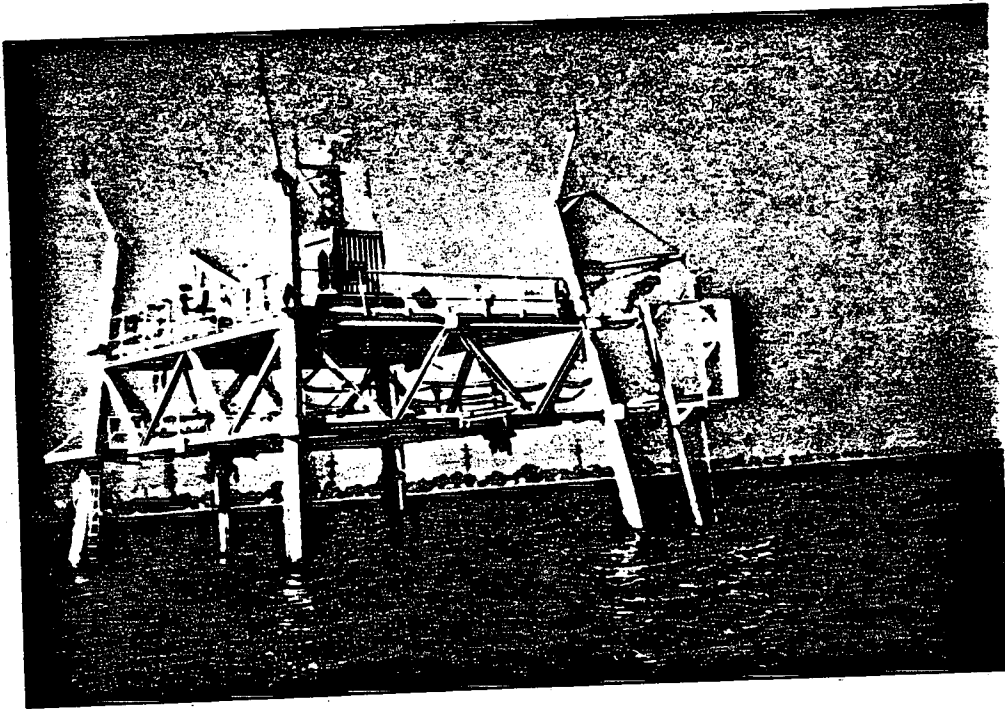


Figure 3

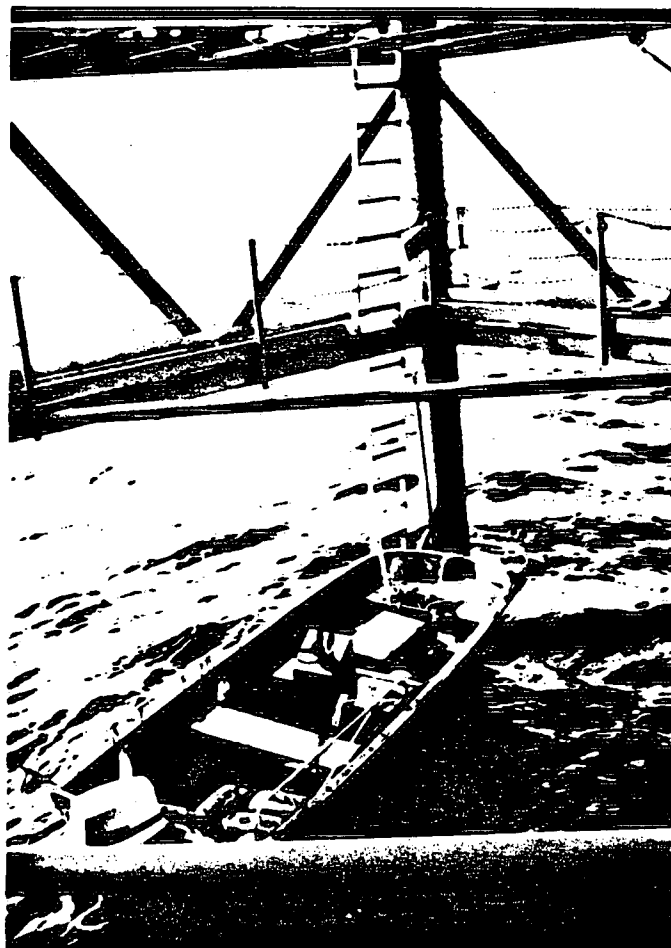


Figure 4

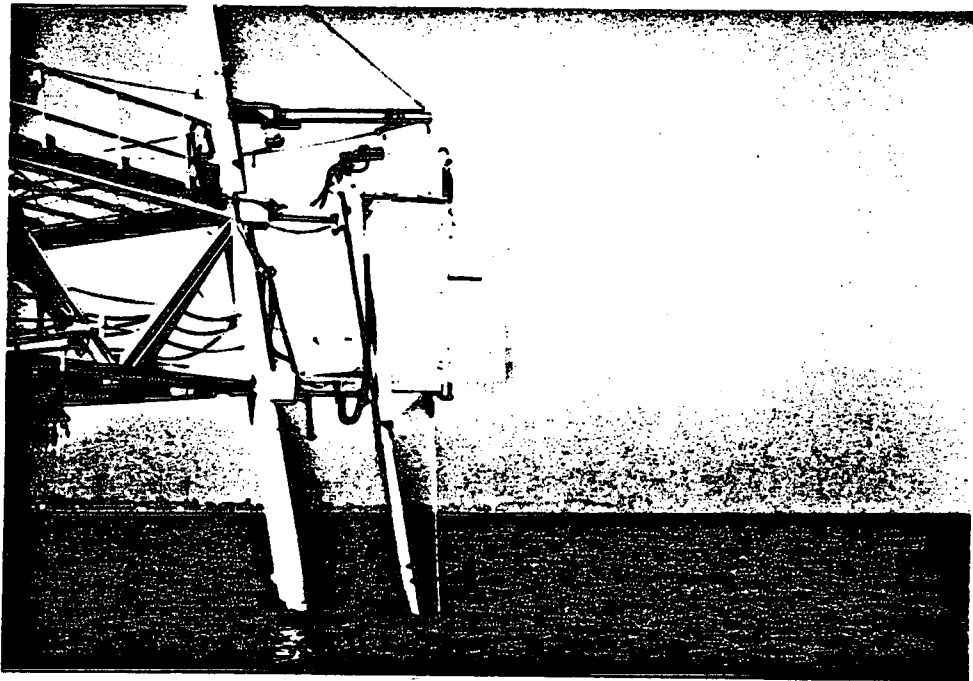


Figure 5

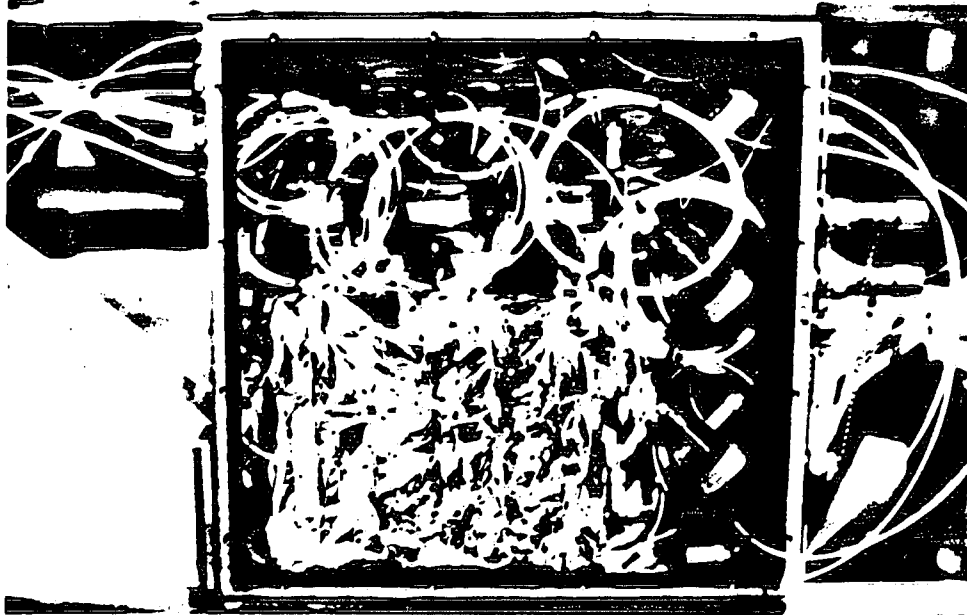


Figure 6



Figure 7

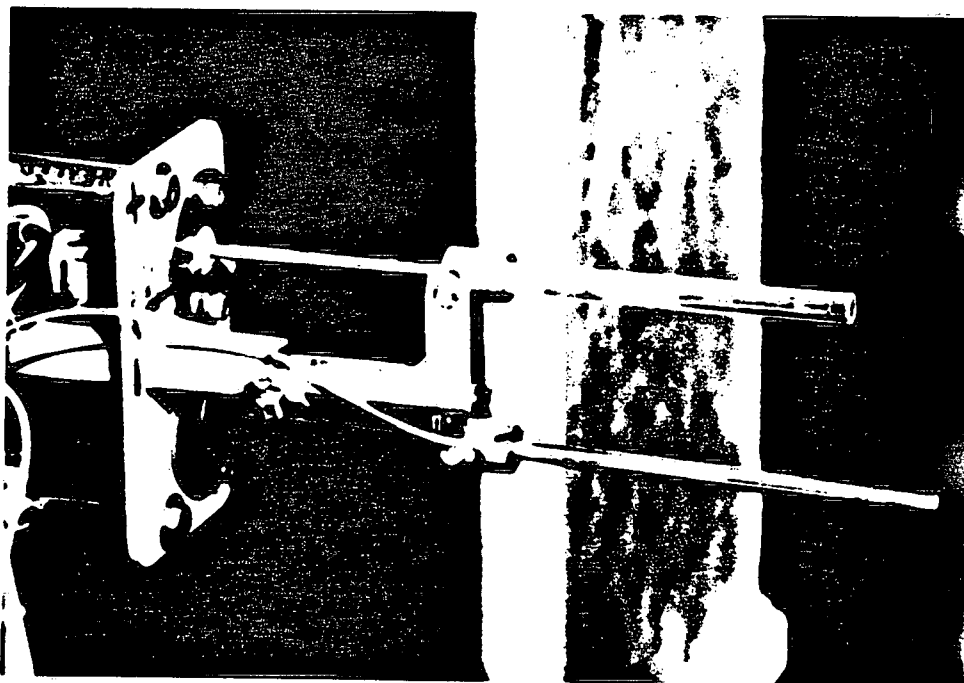


Figure 8

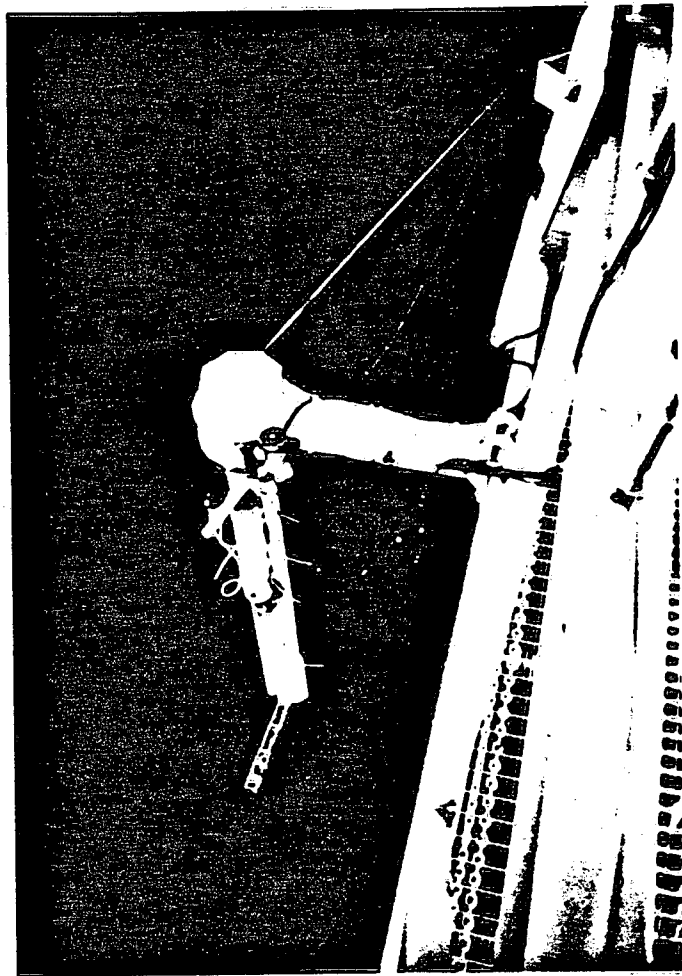


Figure 9

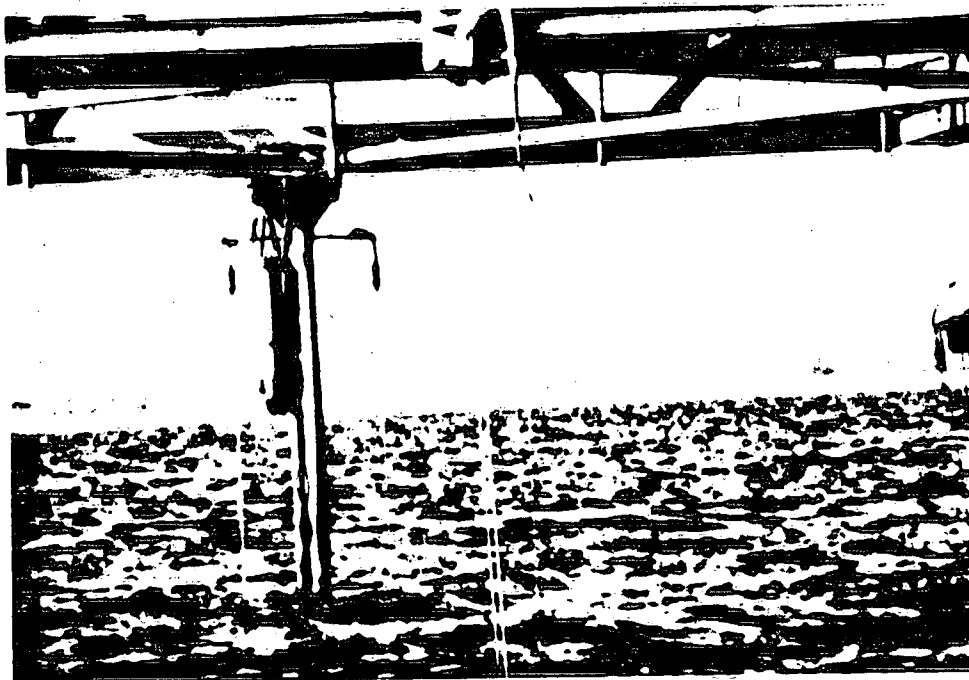


Figure 10

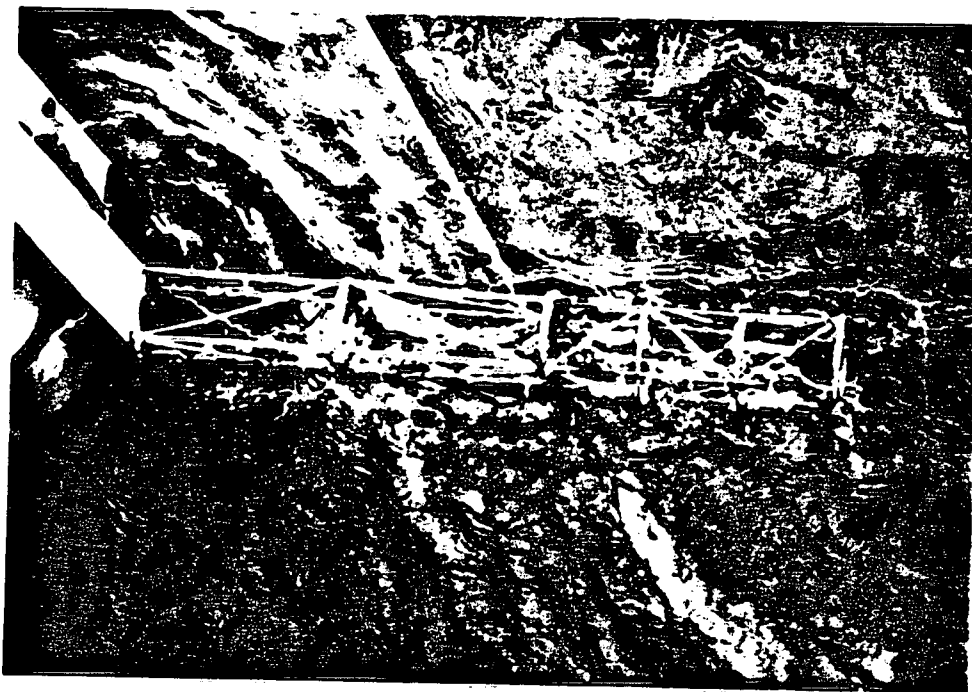


Figure 11

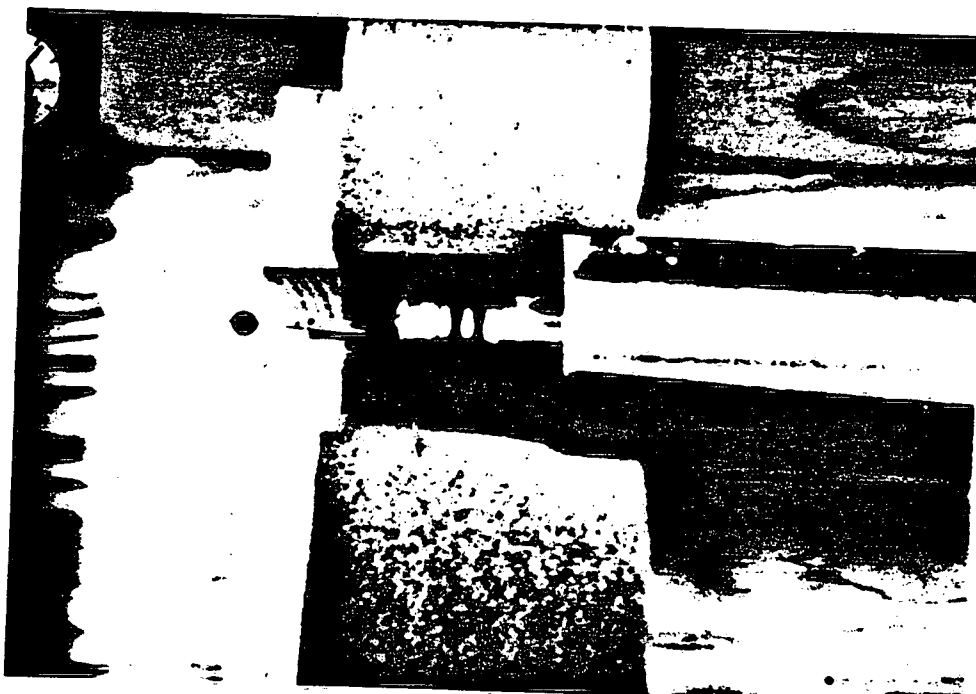


Figure 12



Figure 13

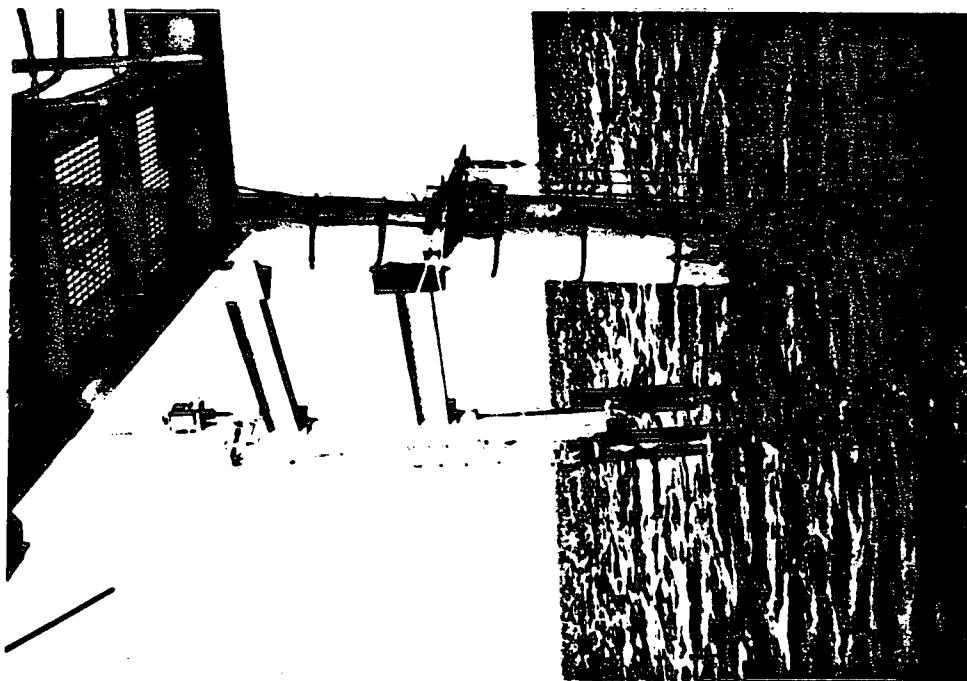


Figure 14

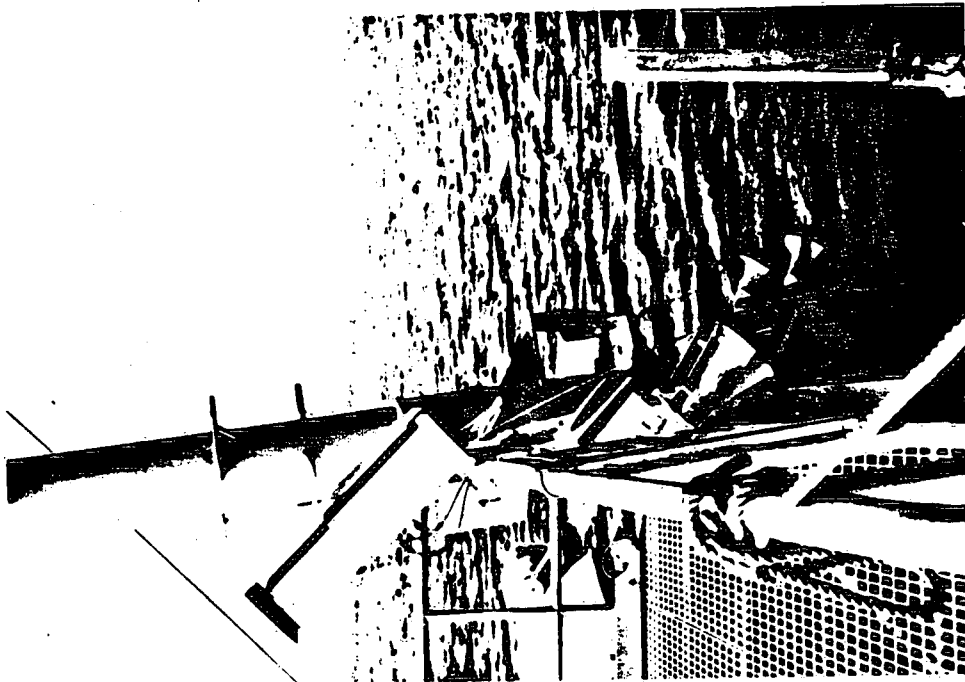


Figure 15

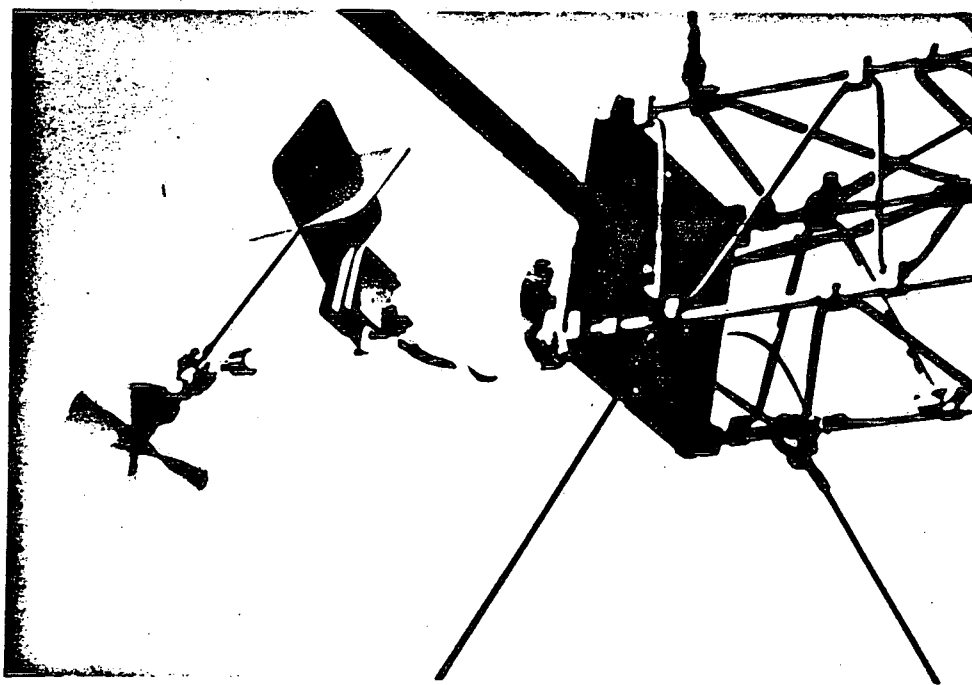


Figure 16

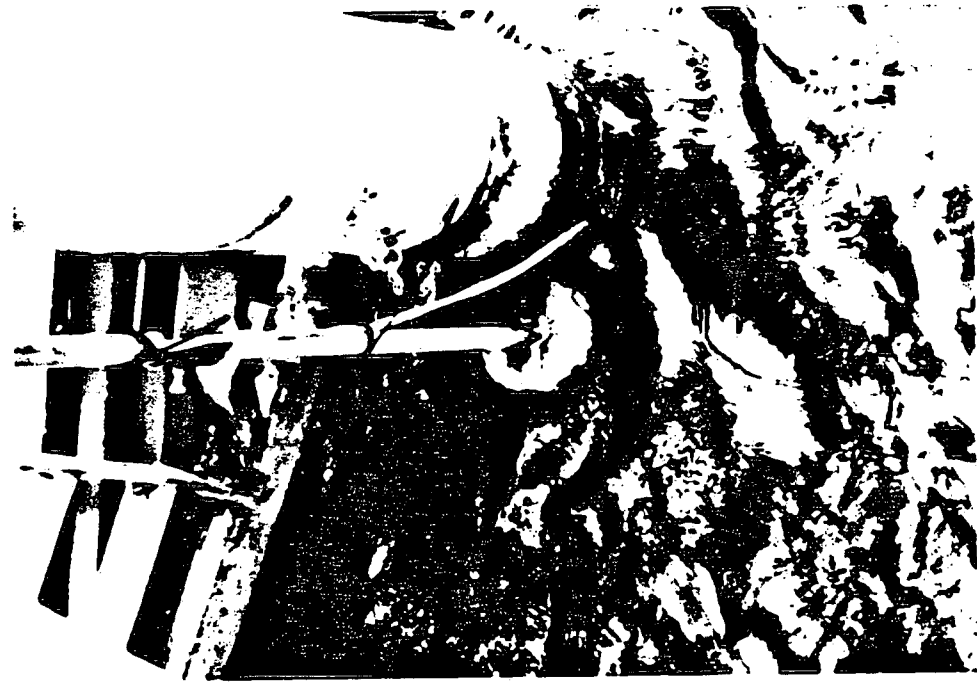


Figure 17

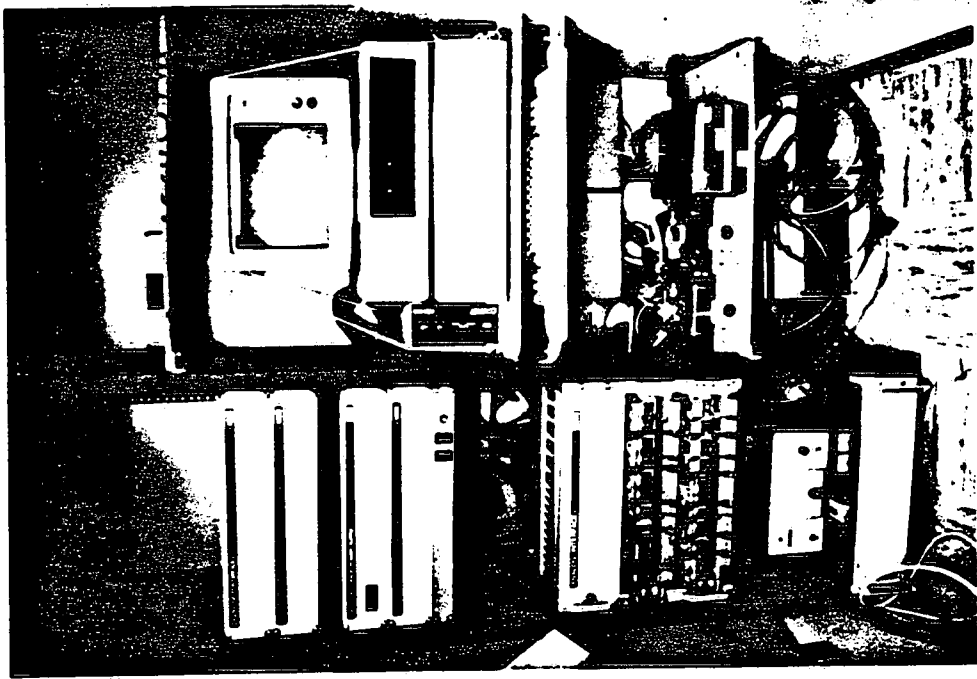


Figure 18



Figure 19



Figure 20

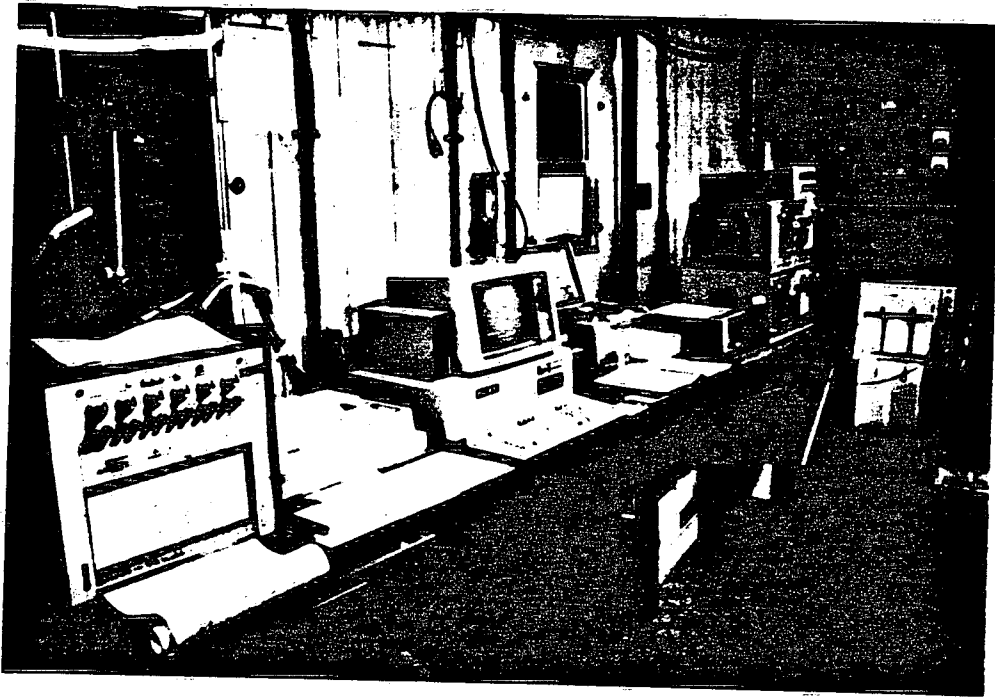


Figure 21

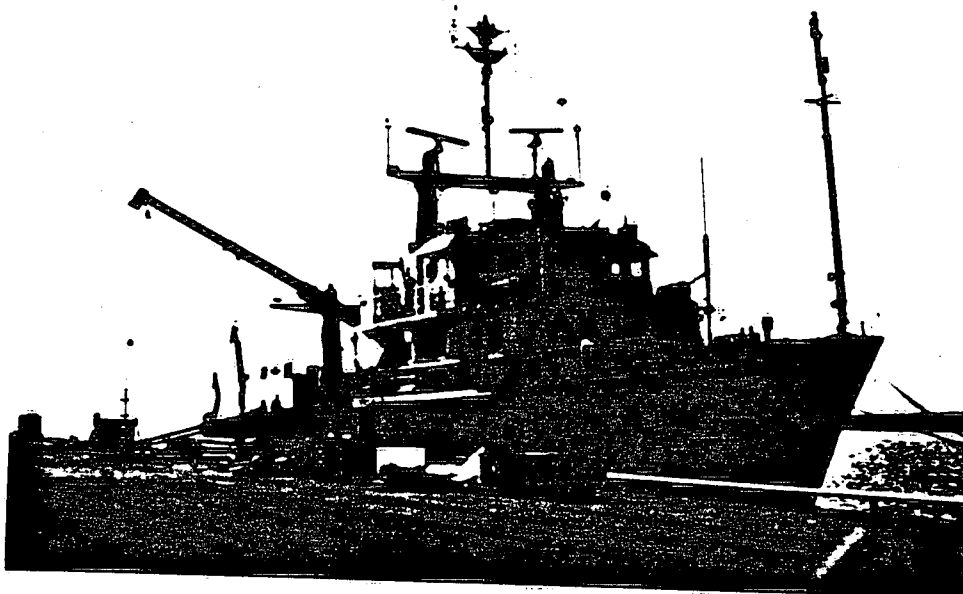


Figure 22

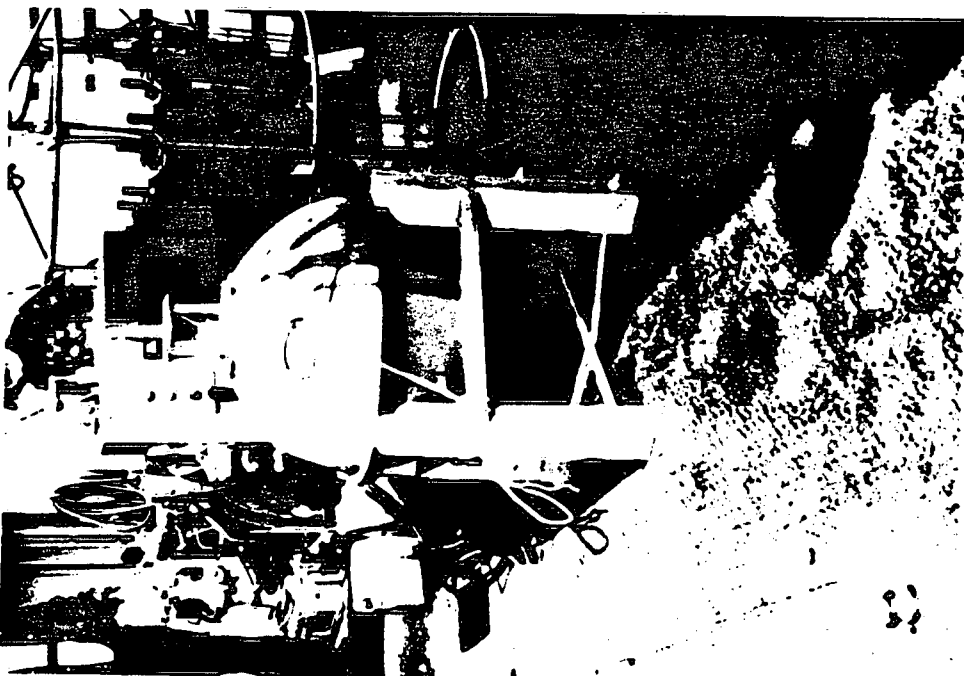


Figure 23

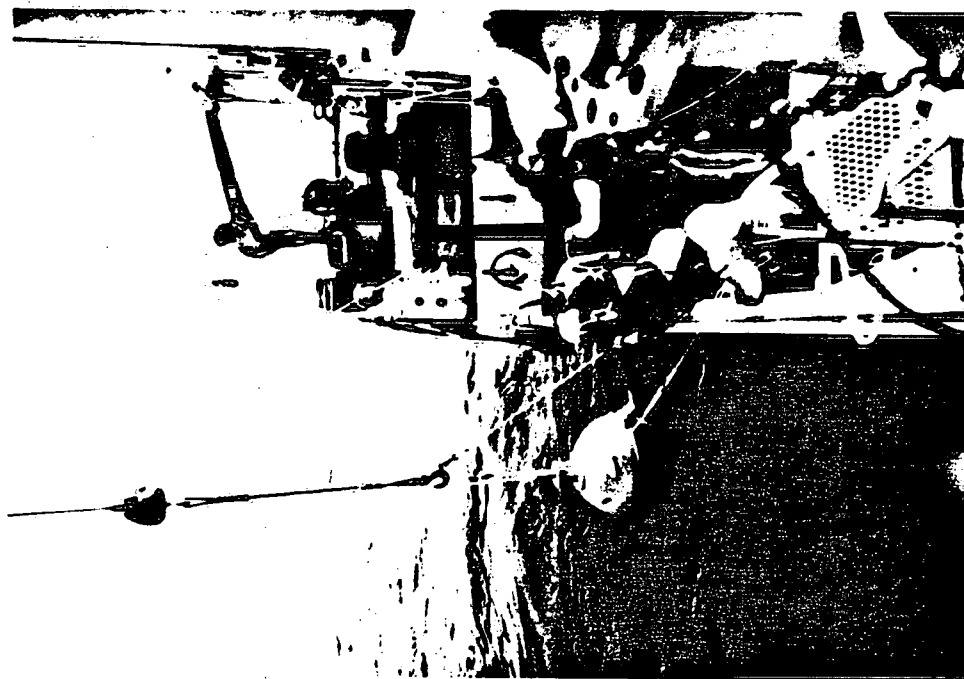


Figure 24



Figure 25



Figure 26

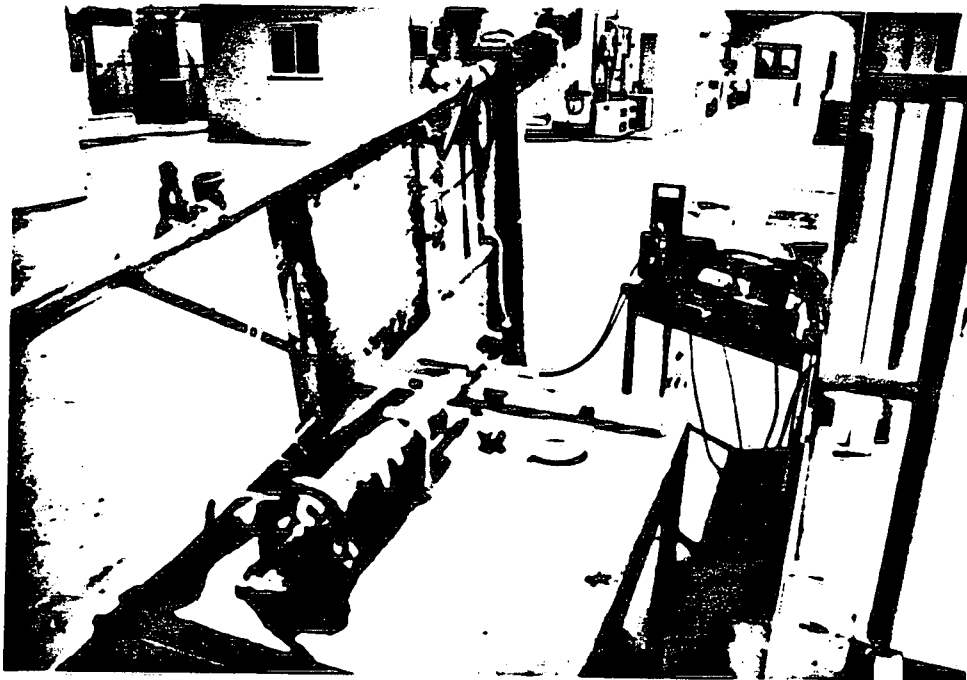


Figure 27

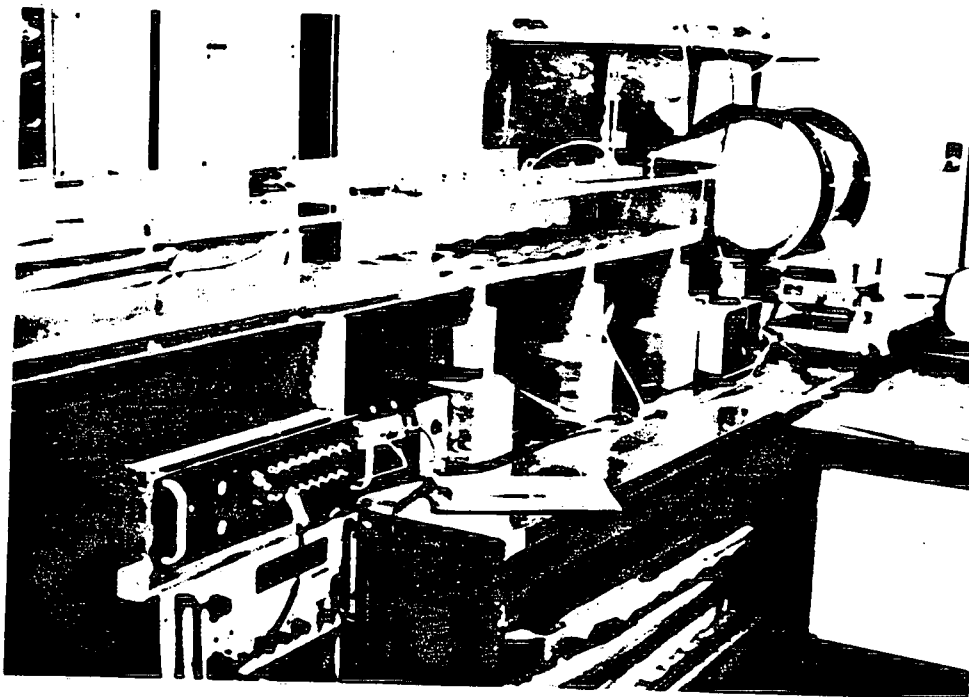


Figure 28

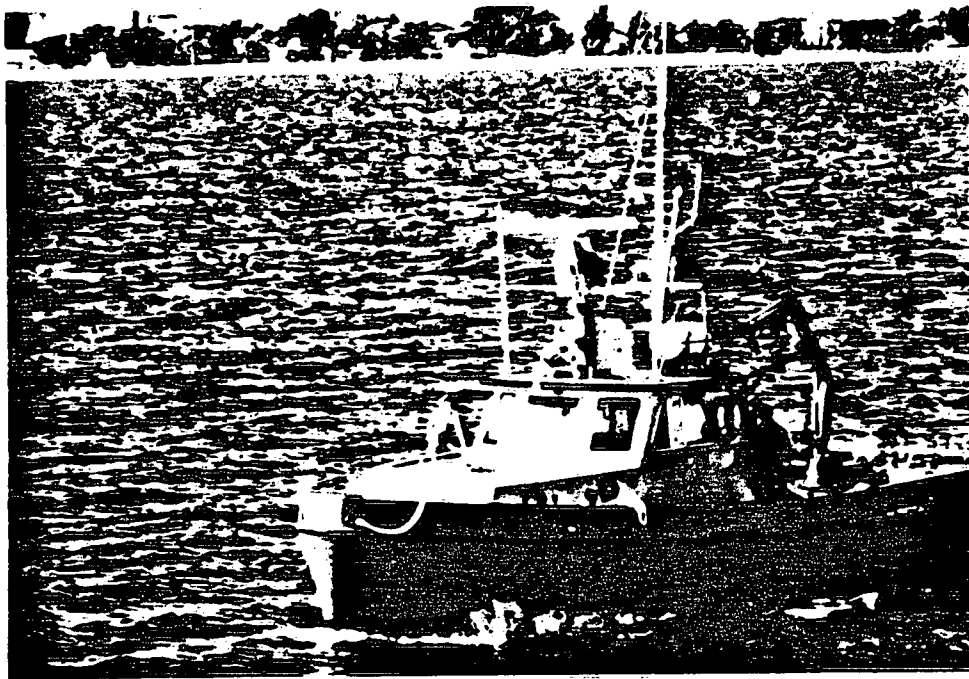


Figure 29

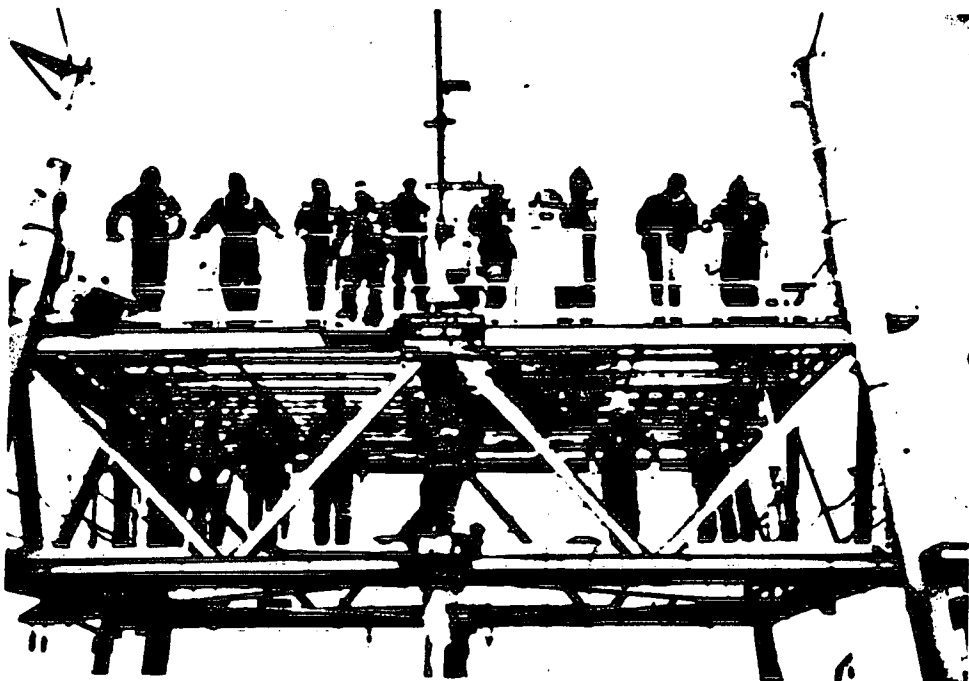


Figure 30

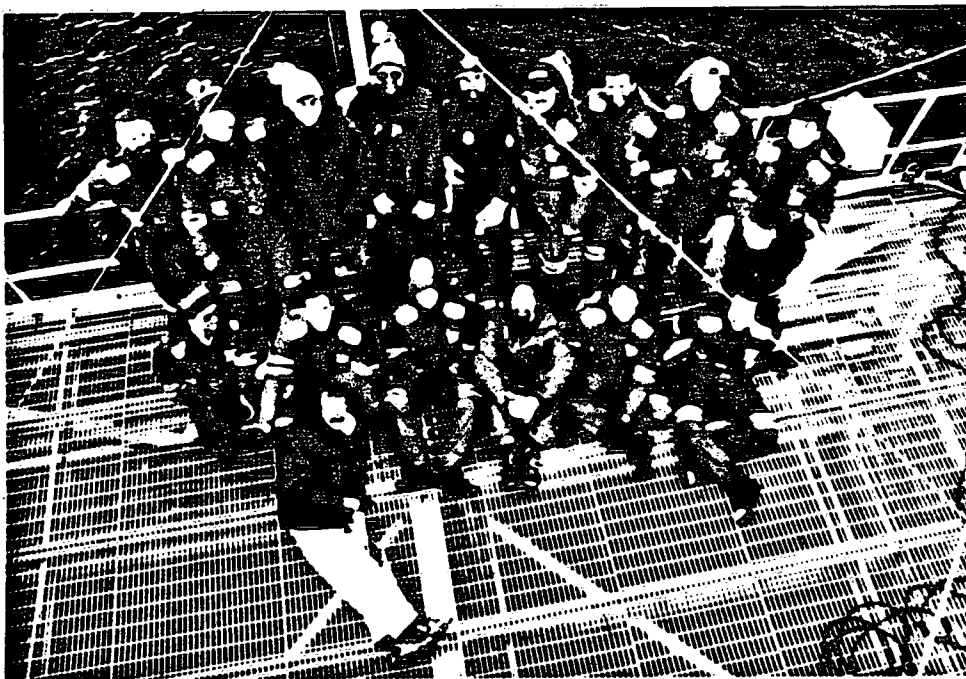


Figure 31



Figure 32